

Probing Local Dynamics of the Photosynthetic Bacterial Reaction Center with a Cysteine Specific Spin Label

Oleg G. Poluektov,* Lisa M. Utschig, Sergio Dalosto, and Marion C. Thurnauer

Chemistry Division, Argonne National Laboratory, Argonne, Illinois 60439

Received: January 29, 2003; In Final Form: April 22, 2003

A multifrequency electron paramagnetic resonance (EPR) approach was used to probe the dynamic structure of the bacterial photosynthetic reaction center (RC) protein. We have demonstrated that the cysteine specific nitroxide spin label MTSL can be covalently bound to a surface cysteine residue of *Rhodobacter sphaeroides* RC protein. We suggest that the MTSL nitroxide is bound to an accessible cysteine residue, H156, which is located on the surface of the protein on the H-subunit. Analysis of the multifrequency EPR spectra of the spin-labeled RC proteins suggests the restricted character of the protein dynamics. These dynamics can be described as fast libration in a cone with a correlation time faster than 10^{-9} s. Several dynamically nonequivalent sites were observed in the EPR spectra, which may reflect distinct conformational substates of local protein structure. This work provides a foundation for future studies with the goal of correlating protein motions with photosynthetic charge-transfer reactions.

1. Introduction

The structure of biomolecules is dynamic at physiological temperature, fluctuating between different conformational substates.^{1–4} In proteins, this intrinsic conformational flexibility is often critical for biological function.^{5,6} Recent studies have highlighted the role of protein dynamics in promoting electron transfer.^{7–12} Thus, methods to directly discern the connection between protein motion and electron-transfer events are required to understand protein functioning.

There is strong evidence that electron transfer in the photosynthetic bacterial reaction center protein (RC)[†] is governed by conformational changes. Thus, the crystallographically characterized RC^{13–15} provides a useful native system to explore the nature of protein motion coupled to biological electron transfer. The RC is an integral membrane protein that facilitates the conversion of light energy to chemical energy. Three polypeptides, the L, H, and M subunits, form this protein complex, binding nine cofactors: four bacteriochlorophylls (Bchl), two bacteriopheophytins (Bph), two ubiquinones (Q), and one non-heme iron. Upon absorption of a photon by a “special” pair of bacteriochlorophyll molecules (P), electron transfer occurs sequentially through the set of cofactors, terminating in the electron transfer between quinone cofactors, Q_A and Q_B.

Several studies of the *Rhodobacter (Rb.) sphaeroides* RC reveal that conformational changes accompany some of the electron-transfer reactions. The electron transfer between Q_A and Q_B is temperature activated^{16–18} and coupled to proton movement.^{19,20} Importantly, the first interquinone electron transfer is believed to be a conformationally gated process,^{11,21,22} where the protein dynamics control the rate of reaction.²³

However, a detailed mechanism for the involvement of protein dynamics in this electron-transfer event is not known. Heterogeneous kinetics observed for Q_A to Q_B electron transfer at room temperature indicate that the RC structure is distributed around configurations that result in fast and slow electron transfer.^{16,18} At low temperature, the appearance of distributed kinetics indicates the freezing in of the conformational substates.¹⁶ Alteration of reaction kinetics by illumination while cooling has been linked to the trapping of reaction centers in altered conformations induced by charge separation.²⁴ A study of several trapped conformational substates along the reaction coordinate has been recently reported.¹²

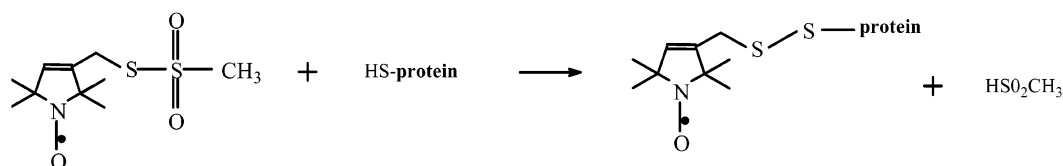
One approach to probing molecular dynamics involved in these conformational changes linked to electron transfer is to study site-specific spin-labeled RCs. Electron paramagnetic resonance (EPR) studies of spin-labeled proteins are capable of providing detailed information about global protein dynamics and local mobility of specific sites within a protein.^{25,26} Most of the dynamical studies are based on stable nitroxide radicals as spin label molecules.²⁷ Anisotropy of hyperfine and spin-orbit interactions make the resonance field of these radicals orientation dependent. Therefore, reorientation of nitroxides causes changes in their EPR spectral shapes. Analysis of these line shape changes allows elucidation of protein dynamics. The spin-labeling technique becomes especially advantageous when carried out with EPR at high-magnetic fields. Enhancement of the spectral resolution of the high-frequency EPR reveals unique information on the motional anisotropy and the mechanism of the molecular reorientation.^{28–34} High-frequency EPR is especially effective for the slow motion region where the structure of the EPR spectra is close to that of the “rigid limit” spectrum, and all main components of the g-tensor are well resolved.

The recent development in the site-directed mutagenesis method has provided additional momentum to the application of spin-labeling techniques to protein studies. By combining cysteine-substitution mutagenesis with cysteine specific methanethiosulfonate labeling (MTSL), nitroxide can be covalently bound to any desired site in a protein. The structural formula

* Corresponding author. Address: Chemistry Division D-200, Argonne National Laboratory, 9700 S. Cass Ave., Argonne, IL 60439. Phone: (630) 252-3546. Fax: (630) 252-9289. E-mail: poluektov@anchem.chm.anl.gov.

† List of abbreviations: RC, reaction center; Rb., *Rhodobacter*; EPR, electron paramagnetic resonance; Bchl, bacteriochlorophyll; Bph, bacteriopheophytin; Q, quinone; P, special pair of chlorophylls; MTSL, [(1-oxyl-2,2,5,5-tetramethylpyrrolin-3-yl)methyl]ethanethiosulfonate spin label; SRLS, slow relaxing local structure; MOMD, microscopic order macroscopic disorder.

SCHEME 1



of the MTSL used in our study and the specific reaction with cysteine residue is shown on Scheme 1.

However, if the protein has only one or a few cysteine residues, the MTSL label can be used without time-consuming mutagenesis. Inspection of the structure of the photosynthetic RC protein from *Rb. sphaeroides* shows that there are five cysteine residues at positions L92, L108, L247, H156, and H234. The cysteine residue at H156 is located on the surface of the protein, as observed in the crystal structure.^{13–15} The other four cysteines are more than 10 Å from the surface. Previous studies have shown one unique surface-accessible cysteine, H156,³⁵ is reactive with thiol reactive derivatives of biotin, rhodamine,³⁶ and fluorescein.³⁷

The aim of this work is to clarify the possibility of covalently binding a cysteine specific spin label to the surface accessible cysteine residue H156 and to obtain parameters of the protein dynamics. These studies provide a benchmark for future work that will probe conformational dynamics at the different sites of the protein and correlate these dynamics with electron and proton-transfer kinetics. This correlation is important for understanding the role of the polypeptide structure in RC function. To make such a correlation, it is very important to extract reliable dynamic parameters from the experimental data. The complex dynamics of spin-labeled proteins include overall isotropic tumbling of the globular protein, fluctuation of specific protein side chains, and spin label reorientation with respect to alkyl side chains. Dissecting these types of complex dynamic modes from EPR spectra provides quite a challenge. We believe that the simultaneous fitting of multifrequency EPR spectra of spin-labeled proteins is important for discriminating between different dynamical modes of motion. Thus far, a cohesive, single model for the simultaneous analysis of multifrequency EPR spectra from nitroxide spin-labeled proteins has not been developed and we expect our work will also contribute to developments in this area.

Herein, we report the first X-band (9.5 GHz) and D-band (130 GHz) EPR characterization of spin-labeled photosynthetic RC proteins. We prove that cysteine specific methanethiosulfonate nitroxide radical can be covalently bound to the bacterial RC protein. A multifrequency approach to the analysis of the temperature-dependent EPR spectra demonstrates the restricted character of the spin label dynamics. These motions can be described as a very fast libration in a cone, the angle of which is increased with temperature. The correlation time of this motion is faster than 10^{-9} s. This work provides a foundation for future studies with the goal of correlating protein motions with photosynthetic charge-transfer reactions.

2. Material and Methods

2.1. Spin-Labeling the Bacterial RC. RCs from the photosynthetic bacterium *Rb. sphaeroides* R-26 were isolated as previously described.³⁸ Protein concentrations were determined with the extinction coefficient $\epsilon_{802} = 288 \text{ mM}^{-1} \text{ cm}^{-1}$.³⁹ [(1-Oxyl-2,2,5,5-tetramethylpyrrolidin-3-yl)methyl]methanethiosulfonate spin label (MTSL) was obtained from Reanal (Budapest). RCs ($\text{OD}_{802} = 140 \text{ cm}^{-1}$, $A_{280}/A_{802} = 1.25$ in 10 mM Tris–

HCl, pH 7.86, 0.01 mM EDTA, 280 mM NaCl, and 0.045% lauryldimethylamine *N*-oxide) were incubated with 0.9 mol equiv MTSL per RC and tumbled for 4 h at 4 °C in the dark. MTSL was added from a 14.4 mM stock solution prepared in acetonitrile, resulting in 3% v/v final concentration acetonitrile in the protein buffer detailed above. Glycerol was not added to the RC samples prior to EPR measurements. The RCs (480 μM) were not concentrated further after addition of the spin label. The UV–vis absorption spectrum of the RC remained unchanged after it had undergone the above procedure.

2.2. EPR Spectroscopy. Continuous wave X-band data were collected on a commercial Bruker EPR300E EPR spectrometer with a Bruker X-band ER046XK-T bridge. High-frequency EPR spectra were recorded with a home-built D-band (130 GHz/4.6 T) continuous wave/pulsed EPR spectrometer previously described.⁴⁰ A cylindrical single mode cavity TE₀₁₁ was used for the spectral recording. For precise calibration of the magnetic field, a reference sample was placed in the cavity together with the sample under study. The *g*-value of the reference Mn^{2+} signal was calibrated using an aqueous solution of Fremi salt. This radical has narrow EPR lines and its magnetic resonance parameters were measured with high accuracy at X-band EPR: $g_{\text{iso}} = 2.00550 \pm 0.00004$, $A_{\text{iso}} = 13.091 \pm 0.004 \text{ G}$.⁴¹ Without taking into account second-order terms, the effective *g*-value (middle between third and fourth hyperfine components) and effective hyperfine splitting (splitting between third and fourth hyperfine components) for Mn^{2+} were determined as $g_{\text{eff}} = 2.00122 \pm 0.00004$, $A_{\text{eff}} = 86.7 \pm 0.1 \text{ G}$.⁴²

At the X- and D-band, the sample temperature was regulated by an Oxford temperature controller (ITC 503) coupled to an Oxford continuous flow cryostat (CF 1200). Simulation programs developed in the group of Prof. J. Freed, Cornell University, were used for theoretical fitting of the spectra.⁴³

3. Results and Discussion

The temperature-dependent X-band EPR spectra of RCs labeled with the thiol-reactive nitroxide MTSL are shown in Figure 1. At temperatures below 100 K the line shape of the EPR spectrum corresponds to the “rigid limit” spectrum of the nitroxide. This is a spectrum whereby the reorientation processes of the nitroxide radical are very slow and do not contribute to the EPR line shape. When the temperature is increased, a narrowing and shift of the spectral extremes are observed, as well as the appearance of an overlapping isotropic three line spectrum. This narrow triplet corresponds to the “fast motion” spectrum of the nitroxide resulting from unbound MTSL. The ratio of the unbound label was estimated from the relative spectral intensity to be $\sim 2\%$. The fact that spectra recorded at room temperature are still in the slow motion region, is consistent with MTSL reacting with a cysteine residue of the photosynthetic reaction center in a selective manner. To prove that MTSL is covalently bound to the RC, we obtained the EPR spectrum of a solution of RC and TEMPO (2,2,6,6-tetramethylpiperidine-1-oxyl) nitroxide radical. Unlike MTSL, TEMPO does not have any specificity for the direct labeling of amino acids. The sample was prepared under the same conditions as

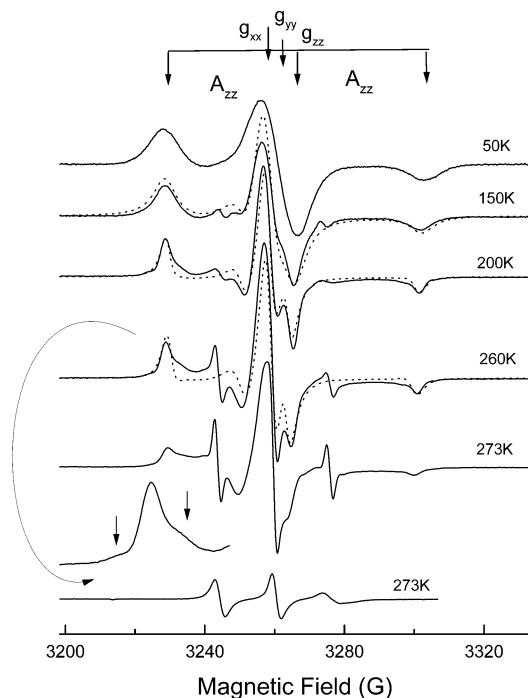


Figure 1. Temperature dependence of the X-band spectra of the bacterial RC labeled by MTSL. The bottom spectrum was recorded from a protein solution, which was incubated with 0.9 mol equiv of TEMPO label per rc. The low-field part of the spectrum recorded at 260 K is enlarged in the lower-left corner; arrows indicate the positions of the extra peaks. The dotted lines are fits with the Brownian diffusion model. Magnetic resonance parameters used for simulations of the EPR spectra are as follows: $g_x = 2.00831$, $g_y = 2.00612$, $g_z = 2.00232$, $A_x = A_y = 5.5$ G, $A_z = 37.4$ G. Arrows at the top show approximate positions of the canonical peaks.

the MTSL sample, but the concentration of TEMPO was taken 10 times lower. Only a narrow isotropic triplet, which is characteristic for unbound, fast rotating nitroxide, was observed in this case (Figure 1). This result shows that MTSL is covalently bound to the RC and not simply adsorbed to the protein surface.

Interestingly, the outer extremes of the spectra reveal heterogeneity in molecular mobility. As seen in the inset of Figure 1, the low-field extreme has shoulders on both sides. Three different possibilities could explain the observed heterogeneity; different binding sites, protein–protein interactions, or different conformations of the protein. Although we cannot definitely rule out the first possibility of multiple binding sites, we feel it is unlikely due to the substoichiometric binding of MTSL in the sample preparation (0.9 mol equiv MTSL/1.0 RC). Although *Rb. sphaeroides* RCs have five cysteine residues, only one cysteine residue at H156 is located on the surface of the protein. The other four cysteines are more than 10 Å from the surface. On the basis of this observation and previous studies, which have shown one unique surface-accessible cysteine,^{35–37} we believe that the MTSL is bound at one surface accessible cysteine, H156, on the H-subunit.

To check the second possibility of protein–protein interactions, we measured the concentration dependence of the EPR spectra. The line shape of the extremes was exactly the same for the MTSL-labeled protein concentration of 0.5 and 0.1 mM. If the observed heterogeneity were due to the protein aggregation, the EPR line width would depend on concentration.

We propose that the heterogeneity of the spectra may reflect distinct conformational substates of local protein structure. In

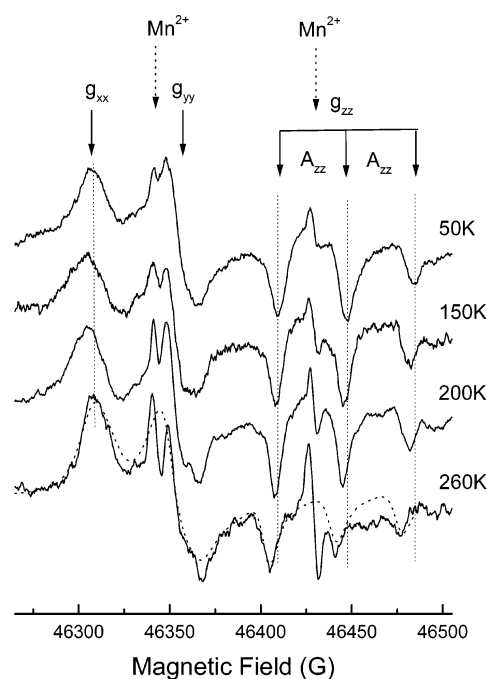


Figure 2. Temperature dependence of the D-band spectrum of the bacterial RC labeled by MTSL. The dashed line is a fit with the Brownian diffusion model. Magnetic resonance parameters used for the fitting are the same as in Figure 1. Dotted arrows at the top indicate positions of the Mn^{2+} lines.

general, proteins exist in several conformational substates along the reaction coordinate, each having different transition temperatures.^{1,2} At low temperatures, a protein's structure is confined and harmonically oscillates near the conformation that it is frozen into. Freezing-in of conformational states has been demonstrated for the RC.^{12,24} Optical experiments have shown that a rapid interconversion of substates coupled to electron transfer is a critical feature of the Q_A to Q_B electron-transfer reaction at room temperature.¹⁶ Similar thermal averaging of conformational substates has been seen for reaction dynamics in other proteins.^{1,44} We believe the motion of the spin label, as detected in the spectra, is sensitive to different conformations of the protein, especially the conformational changes located close to the MTSL binding site of cysteine residue H156. Future experiments with deuterated MTSL-labeled RCs will increase the spectral resolution, hopefully providing further insight into the observed effect.

Due to the presence of the heterogeneity in the molecular mobility and admixture of the unbound spin label, it was impossible to simulate the exact line shape of the spectra. The overall agreement, however, between the obtained fits using the Brownian diffusion model (dotted lines on Figure 1) and the general spectral features of bound MTSL are quite good.

The temperature dependence of the D-band EPR spectra is shown in Figure 2. In the X-band spectra, the orientation selectivity is low and the outer extremes reveal just one pure Z-canonical orientation (see Figure 1). (Notation of the magnetic axes is standard for nitroxides: the X-axis is along the line connecting N–O molecules, the Z-axis is perpendicular to the plane of the pyrroline ring, and the Y-axis in the plane of the ring.) In contrast, peaks from all three canonical orientations are well-resolved in the D-band spectra. A low-field component corresponds to RCs with the MTSL X-axis of the \mathbf{g} -tensor parallel to the magnetic field. The middle component has a first derivative line shape and corresponds to RCs with the MTSL Y-axis along the magnetic field. The three high-field components

correspond to the RCs with the MTSZ Z-axis along the magnetic field. The nitrogen hyperfine splitting is clearly resolved only in the Z-orientation, resulting in the observed triplet spectrum. The low- and high-field peaks of this triplet correspond to the low- and high-field extremes in the X-band spectrum (see Figures 1 and 2). To measure absolute shifts of the canonical components, the spectra were recorded with a Mn^{2+} reference signal. Dotted arrows indicate two narrow lines from the Mn^{2+} sextet.

Because of the high degree of spectral resolution observed at the D-band, relaxation changes in EPR line shapes can be analyzed in terms of rotational motion of the radicals around different molecular axes. Thus, unique information about molecular motion anisotropy can be obtained by independently following relaxation changes of the X-, Y-, and Z-canonical components. With an increase in temperature, the observed shift of the Z-component is larger than that observed for the X-component (see Figure 2). This indicates an anisotropic molecular motion with the axis of preferable reorientation close to the direction of the X-axis of the \mathbf{g} -tensor. Simulations also demonstrate that motion is anisotropic around the X-axis. The dashed line in Figure 2 displays a satisfactory fit with X-anisotropy parameter $N = 5$, where N is a ratio of rotational correlation times around fast and slow axis of reorientation. Note that even for the high-temperature data, the spectral simulations are not unique and a similarly satisfactory fit can be obtained using a different set of parameters; however, this does not change the conclusion that anisotropic motion occurs around the X-axis. The main reason for the spread in the fitting parameters is the poor signal-to-noise (S/N) ratio of the experimental data. Deuteration of our system will increase the S/N and allow us to follow the relaxation changes in the line shape more precisely.

All our attempts to simultaneously fit the D- and X-band spectra with the same set of parameters failed. The correlation times for simulation of the D-band spectra are approximately 2 times shorter than for the corresponding X-band spectra. This effect has been reported before for the simulation of D- and X-band EPR spectra of a spin-labeled polymer⁴⁵ and spin probes in vitrified isotropic solutions.⁴⁶ The effect has been explained by the presence of "fast" restricted oscillations (librations) of the molecule in the "slow" relaxing surroundings.

To demonstrate the observed differences, we plotted a correlation curve of the relative shifts for X-band and D-band spectra (Figure 3).^{45,46} The parameters R and r are defined in the inset in Figure 3. R_0 and r_0 are splittings between external extremes for rigid limit spectra at the D- and X-band, respectively. The experimental curve in Figure 3 has a lower slope than the theoretical curves calculated for both isotropic and anisotropic rotation around the Y-axis for the cases of Brownian (dashed) and jump (dotted) reorientational models.⁴³ Theoretical curves for anisotropic motion around the X- or Z-axis will make this discrepancy even larger. There is no crossing between theoretical and experimental curves, thus Brownian or jump diffusion cannot explain D- and X-band spectra simultaneously.

The detailed explanation of this observation, that correlation times for simulation of the D-band spectra are approximately 2 times shorter than for the corresponding X-band spectra, has been discussed before.^{45,46} Recording the spectra of nitroxide radicals at higher frequencies leads to an increase in the magnetic anisotropy of the spectra, i.e., frequency range averaged by the reorientation motion. Depending upon the mechanism, an increase in the spectral anisotropy can have different effects on the relaxation shifts of the canonical

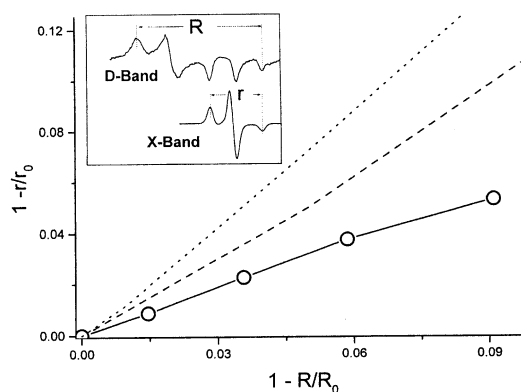


Figure 3. Correlation of the dependence of the relative shifts for X-band ($1 - r/r_0$) and D-band ($1 - R/R_0$) spectra of the bacterial RC labeled by MTSZ. Circles: experimental data. Dashed line: theoretical curve calculated with the Brownian diffusion model for the cases of isotropic and anisotropic rotation around the Y-axis. Dotted line: the same theoretical curve, but for the case of jump diffusion for big angles. Parameters R and r are defined on the inset.

components. Thus, for Brownian diffusion this shift is proportional to the square root of the averaged anisotropy.⁴⁷ For a jump diffusion through a big angle the shift even decreases with increasing anisotropy.⁴⁸ However, absolute shifts observed experimentally have an almost linear dependence upon the magnetic anisotropy. To explain this dependence, we have to assume that the spin label undergoes fast reorientation within a restricted angle or cone. In this case, a shift of the canonical component will be determined by the averaging of the resonance fields within the cone and can be written as

$$\delta H(\theta) = \alpha \langle \sin^2(\theta) \rangle \quad (1)$$

where θ is the angle of deviation from the canonical orientation (libration angle) and $\alpha = (\partial^2 H / \partial \theta^2)_{\theta=0}$ is a magnetic anisotropy parameter.

Recently, the same observation has been reported in the multifrequency EPR studies of a spin-labeled protein³⁰ and polymer.²⁹ These authors found that, to fit the 250 GHz spectra, the relaxation rates should be 4 times shorter than for the 9 GHz spectra. This problem was resolved by simulating X-band spectra within a slow relaxing local structure (SRLS) model, whereas the 250 GHz spectra were simulated with a microscopic order, macroscopic disorder (MOMD) model.

The model of librations (originally termed "wobble model"⁴⁹) is well accepted for describing anisotropic media, such as spin-labeled polymer molecules, where restriction of the angular amplitudes is determined by the flexibility of the connecting bonds^{50–52} and liquid crystals, where the concept of the relaxation of local structure has been introduced to account for fast restricted oscillations.^{53,54} There is strong indication that the libration model accounts for reorientation in isotropic media as well.^{46,55,56} A recent spin probe study of mobility in isotropic media by the method of oriented spin probe unambiguously proves that the libration model is general for molecular reorientation.⁵⁷ It was shown that restricted librations (fast motion mode) are 10 orders of magnitude faster than slow unrestricted relaxation of the surroundings (slow motion mode). Furthermore, it was argued that the difference between the libration model and SRLS is that in SRLS the fast mode is only an order of magnitude faster than the slow mode, which contradicts the experimental results from their system.⁵⁷

On the basis of eq 1 we were able to obtain the angle of librations, θ , as a function of temperature (Figure 4). The angles

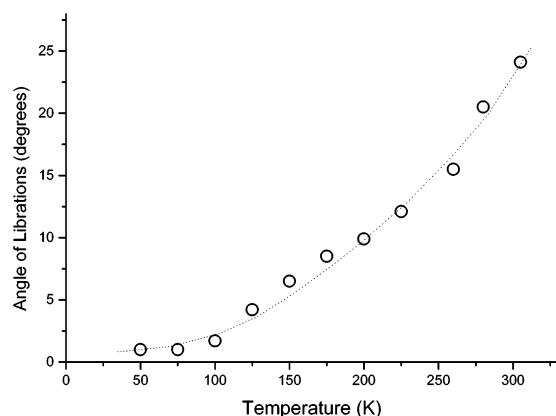


Figure 4. Temperature dependence of the libration angle, θ , for MTSL spin label covalently bound to the bacterial RC. Angle θ is defined in eq 1.

calculated from the shifts of the external extremes in D- and X-band, and averaging of the A_{ZZ} components in the D-band spectra were within 15% of each other. (Figure 4 represents average data of these calculations.) This is another confirmation that reorientational motion is fast libration and contribution of the slow mode, if any, is negligible.

If contribution of the slow mode is negligible, then the observed broadening of the canonical components must be due to incomplete averaging by fast librations.^{46,55–57} From here we can estimate a correlation time, τ , for the fast libration. The line broadening is proportional to $(\delta H(\theta))^2 \tau$. Estimations for different temperatures show that the correlation time τ ranges from 10^{-9} to 10^{-10} s, and line-broadening, as a function of temperature, is mainly determined by the increase of the amplitude of oscillations, $\delta H(\theta)$, but not a correlation time. If the overall unrestricted reorientation is indeed 10 orders of magnitude slower, as it was found in ref 57, then for our case we have to assume a slow mode correlation time on the order of seconds. Such slow dynamics cannot be manifested in the EPR spectra. At any rate, our estimation of 10^{-9} s should be considered as a high limit for the libration correlation time. Interestingly, libration mobility is observed at a temperature as low as 100 K (see Figure 4), indicating that the protein has a flexible structure.

The sulfur atom of the RC's H-subunit surface accessible cysteine, H156, to which the MTSL is evidently bound, is located about 29 Å from the headgroup of Q_A and 37 Å from Q_B . The H-subunit contains the putative site for proton entry into the RC, for delivery to Q_B .⁵⁸ This site might coincide with a metal binding site on the RC,⁵⁹ which is in the vicinity of cysteine H156. Interestingly, when a metal binds to this site local protein dynamics, important for electron transfer in the RC, is altered.^{59–61} Thus we expect that the data presented here will shed light on the proton coupled electron-transfer process.

4. Conclusion

Herein, we report the first X-band (9.5 GHz) and D-band (130 GHz) EPR characterization of a spin-labeled photosynthetic RC protein. We have demonstrated that the cysteine specific nitroxide spin label MTSL can be covalently bound to the bacterial RC protein. We suggest that the MTSL nitroxide is bound to an accessible cysteine residue, H156, which is located on the surface of the protein on the H-subunit, whereas four other available cysteines are more than 10 Å from the surface. Analysis of the multifrequency EPR spectra of the spin-labeled RC suggests the restricted character of the protein dynamics.

These dynamics can be described as fast libration in a cone with a correlation time faster than 10^{-9} s. The angle of the cone increases with temperature and can be easily obtained from the EPR spectra of the spin-labeled protein. Local dynamics were observed at a temperature as low as 100 K. This type of dynamical behavior is typical for the conformational flexibility observed in other proteins.⁶² Characterization by the libration model satisfactorily describes the multifrequency data. Other common models cannot adequately simultaneously describe both the low- and high-frequency data. As with any emerging field, the validity of the libration model will be tested as more experimental high-field EPR data becomes available.

Future studies will focus on correlating the observed dynamics with photosynthetic electron and proton-transfer events. The multifrequency EPR study of spin-labeled RCs presented herein has the potential to be sensitive to subtle protein movements involved in dynamic processes of the RC that cannot be observed in the static crystal structure. Protein reorganization energies have been implicated to be important in controlling electron-transfer processes. For instance, experiments have shown that large changes in $P^+Q_A^-$ recombination,^{63,64} Q_A to Q_B electron-transfer rates,¹⁶ or pheophytin to Q_A electron-transfer rates in Fe-removed RCs⁶⁵ can occur without large changes in the donor/acceptor geometries. Using site-directed mutagenesis, cysteine residues could be incorporated into different regions of the RC. This technique has been important in the study of other proteins.⁶⁶ By this method, librations in different regions of the RC can be studied to reveal if the dynamics of different parts of the protein are similar and depend on cooperative motions of protein body as a whole.

Acknowledgment. We thank Prof. J. Freed and Prof. D. Budil for stimulating discussions and for providing their EPR simulation programs. This work was supported by the U.S. Department of Energy, Office of Basic Energy Sciences, Division of Chemical Science, under Contract W-31-109-Eng-38.

References and Notes

- Frauenfelder, H.; Wolynes, P. *Phys. Today* **1994**, 47, 58–64.
- Frauenfelder, H.; Petsko, G. A.; Tsernoglou, D. *Nature* **1979**, 280, 558–563.
- Hartmann, H.; Parak, F.; Steigemann, W.; Petsko, G. A.; Ringe, P.; Drenth, J. *Proc. Natl. Acad. Sci. U.S.A.* **1982**, 79, 4967–4971.
- Parak, F.; Knapp, E. W.; Kuchieda, D. *J. Mol. Biol.* **1982**, 161, 177–194.
- Zaccai, G. *Science* **2000**, 288, 1604–1607.
- Frauenfelder, H.; Sligar, S. G.; Wolynes, P. G. *Science* **1991**, 254, 1598–1603.
- Balabin, I. A.; Onuchic, J. N. *Science* **2000**, 290, 114–117.
- Rabenstein, B.; Matthias Ullmann, G.; Knapp, E.-W. *Biochemistry* **2000**, 39, 10487–10496.
- Davidson, V. C. *Biochemistry* **1996**, 35, 14035–14039.
- Zhou, J. S.; Kostic, N. M. *J. Am. Chem. Soc.* **1993**, 115, 10796–10804.
- Graige, M. S.; Feher, G.; Okamura, M. Y. *Proc. Natl. Acad. Sci. U.S.A.* **1998**, 95, 11679–11684.
- Xu, Q.; Gunner, M. R. *Biochemistry* **2001**, 40, 3232–3241.
- Allen, J. P.; Feher, G.; Yeates, T. O.; Komizy, H.; Rees, D. C. *Proc. Natl. Acad. Sci. U.S.A.* **1988**, 85, 8487–8491.
- Ermiler, U.; Fritzsche, G.; Buchanan, S.; Michel, H. *Structure* **1994**, 2, 925–936.
- El-Kabbani, O.; Chang, C.-H.; Tiede, D. M.; Norris, J.; Schiffer, M. *Biochemistry* **1991**, 30, 5361–5369.
- Tiede, D. M.; Vazquez, J.; Cordova, J.; Marone, P. A. *Biochemistry* **1996**, 35, 10763–10775.
- Mancino, L.; Dean, D.; Blankenship, R. *Biochim. Biophys. Acta* **1984**, 764, 46–54.
- Li, J.; Gilroy, D.; Tiede, D. M.; Gunner, M. R. *Biochemistry* **1998**, 37, 2818–2819.
- Parson, W. W. In *Photosynthesis*; Ames, J., Ed.; Elsevier: New York, 1987; pp 43–61.

- (20) Shinkarev, V. P.; Wraight, C. A. In *The Photosynthetic Reaction Center*; Deisenhofer, J., Norris, J. R., Eds.; Academic Press: New York, 1993; Vol. 1, pp 193–255.
- (21) Graige, M.; Feher, G.; Okamura, M. *Biophys. J.* **1996**, *70*, SUAM4.
- (22) Brzezinski, P.; Okamura, M. Y.; Feher, G. In *The Photosynthetic Reaction Center II*; Breton, J., Vermeglio, A., Eds.; Plenum Press: New York, 1992; pp 321–330.
- (23) Hoffman, B. M.; Ratner, M. A. *J. Am. Chem. Soc.* **1987**, *109*, 6237–6242.
- (24) Kleinfeld, D.; Okamura, N.; Feher, G. *Biochemistry* **1984**, *23*, 5780–5786.
- (25) Borbat, P. P.; Costa-Filho, A. J.; Earle, K. A.; Moscicki, J. K.; Freed, J. H. *Science* **2001**, *291*, 266–269.
- (26) Hubbell, W. L.; Altenbach, C. *Curr. Opin. Struct. Biol.* **1994**, *4*, 566–573.
- (27) Berliner, L. J. *Spin Labeling. Theory and Applications*; Academic Press: New York, 1976.
- (28) Smirnov, A. I.; Belford, R. L.; Clarkson, R. B. In *Biological Magnetic Resonance*; Berliner, L. J., Ed.; Plenum Press: New York, 1998; Vol. 14, pp 83–107.
- (29) Pilar, J.; Labsky, J.; Marek, A.; Budil, D. E.; Earle, K. A.; Freed, J. H. *Macromolecules* **2000**, *33*, 4438–4444.
- (30) Rarnes, J. P.; Liang, Z.; Mchaourab, H. S.; Freed, J. H.; Hubbell, W. L. *Biophys. J.* **1999**, *76*, 3298–3306.
- (31) Poluektov, O. G.; Lubashevskaja, E. V.; Dubinski, A. A.; Grinberg, O. Y.; Antziferova, L. I.; Lebedev, Y. S. *Sov. J. Chem. Phys.* **1989**, *4*, 2683–2689.
- (32) Poluektov, O. G.; Dubinski, A. A.; Grinberg, O. Y.; Lebedev, Y. S. *Sov. J. Chem. Phys.* **1985**, *2*, 30–38.
- (33) Poluektov, O. G.; Dubinski, A. A.; Grinberg, O. Y.; Lebedev, Y. S. *Sov. J. Chem. Phys.* **1984**, *1*, 2500–2516.
- (34) Lebedev, Y. S.; Grinberg, O. Y.; Dubinski, A. A.; Poluektov, O. G. In *Bioactive Spin Labels*; Zhdanov, R. I., Ed.; Springer-Verlag: Berlin, 1992; p 227.
- (35) Debus, R. J.; Feher, G.; Okamura, M. Y. *Biochemistry* **1986**, *25*, 2276–2287.
- (36) Salafsky, J.; Groves, J. T.; Boxer, S. G. *Biochemistry* **1996**, *35*, 14773–14781.
- (37) Osvath, S.; Larson, J. W.; Wraight, C. A. *Biochim. Biophys. Acta* **2001**, *1505*, 238–247.
- (38) Utschig, L. M.; Greenfield, S. R.; Tang, J.; Laible, P. D.; Thurnauer, M. C. *Biochemistry* **1997**, *36*, 8548–8558.
- (39) Straley, S. C.; Parson, W. W.; Mauzerall, D. C.; Clayton, R. K. *Biochim. Biophys. Acta* **1973**, *305*, 597–609.
- (40) Lakshmi, K. V.; Reifler, M. J.; Brudvig, G. W.; Poluektov, O. G.; Wagner, A. M.; Thurnauer, M. C. *J. Phys. Chem. B* **2000**, *104*, 10445–10448.
- (41) Goldman, S. A.; Bruno, G. V.; Polnaszek, C. F.; Freed, J. H. *J. Chem. Phys.* **1972**, *56*, 716–735.
- (42) Grinberg, O. Y. High g-Resolution EPR Spectroscopy. Method and Applications. Thesis Dr. Science, Russian Academy of Sciences, Moscow, 1988.
- (43) Budil, D. E.; Lee, S.; Saxena, S.; Freed, J. H. *J. Magn. Reson.* **1996**, *120*, 155–189.
- (44) Hagen, S. J.; Hofrichter, J.; Eaton, W. A. *Science* **1995**, *269*, 959–962.
- (45) Poluektov, O. G.; Grinberg, O. Y.; Dubinski, A. A.; Sidorov, O. Y.; Lebedev, Y. C. *Teor. Eksp. Khim* **1998**, *4*, 459–466 (Russian).
- (46) Poluektov, O. G.; Grinberg, O. Y.; Dubinski, A. A.; Lukyanenko, L. V.; Sidorov, O. Y.; Lebedev, Y. C. *Russian J. Phys. Chem.* **1988**, *62*, 1067–1070.
- (47) Kivelson, D.; Lee, S. *J. Chem. Phys.* **1982**, *76*, 5746–5754.
- (48) Freed, J. H. In *Spin Labeling. Theory and Applications*; Berliner, L. J., Ed.; Academic Press: New York, 1976; pp 53–132.
- (49) Griffith, H. O.; Jost, P. C. In *Spin Labeling. Theory and Applications*; Berliner, L. J., Ed.; Academic Press: New York, 1976; pp 453–524.
- (50) Johnson, M. E. *Biochemistry* **1978**, *17*, 1223–1231.
- (51) Liang, Z.; Freed, J. H. *J. Phys. Chem. B* **1999**, *103*, 6384–6396.
- (52) Timofeev, V. P. *Mol. Biol.* **1986**, *20*, 697–711.
- (53) Livshits, V. A.; Mares, D. J. *Magn. Reson.* **2000**, *147*, 59–67.
- (54) Polnaszek, C. F.; Freed, J. H. *J. Phys. Chem.* **1975**, *79*, 2283–2306.
- (55) Paschenko, S. V.; Toropov, Y. V.; Dzuba, S. A.; Tsvetkov, Y. D.; Vorobiev, A. K. *J. Chem. Phys.* **1999**, *110*, 8150–8154.
- (56) Dzuba, S. A. *Phys. Lett. A* **1996**, *213*, 77–84.
- (57) Vorobiev, A. K.; Gurman, V. S.; Klimenko, T. A. *Phys. Chem. Chem. Phys.* **2000**, *2*, 379–385.
- (58) Paddock, M. L.; Graige, M. S.; Feher, G.; Okamura, M. Y. *Proc. Natl. Acad. Sci. U.S.A.* **1999**, *95*, 6183–6188.
- (59) Utschig, L. M.; Ohgashi, Y.; Thurnauer, M. C.; Tiede, D. M. *Biochemistry* **1997**, *37*, 8278–8281.
- (60) Utschig, L. M.; Poluektov, O.; Tiede, D. M.; Thurnauer, M. C. *Biochemistry* **2000**, *39*, 2961–2969.
- (61) Utschig, L. M.; Poluektov, O.; Schlesselman, S. L.; Thurnauer, M. C.; Tiede, D. M. *Biochemistry* **2001**, *40*, 6132–6141.
- (62) Likhtenshtein, G. I.; Febbraio, F.; Nucci, R. *Spectrochim. Acta Part A* **2000**, *56*, 2011–2031.
- (63) van den Brink, J. S.; Hulsebosch, R. J.; Gast, P.; Hore, P. J.; Hoff, A. J. *Biochemistry* **1994**, *33*, 13668–13677.
- (64) Franzen, S.; Goldstein, R. F.; Boxer, S. G. *J. Phys. Chem.* **1990**, *94*, 5135–5149.
- (65) Tang, J.; Utschig, L. M.; Poluektov, O.; Thurnauer, M. C. *J. Phys. Chem. B* **1999**, *103*, 5145–5150.
- (66) Hubbell, W. L.; Altenbach, C. *Curr. Opin. Struct. Biol.* **1994**, *4*, 566–573.